GEOPHYSICAL RESEARCH LETTERS, VOL. 23, NO. 8, PAGES 841-844, APRIL 15, 1996

Measurements of upward turbulent ozone fluxes above a subalpine spruce-fir forest

Karl Zeller and Ted Hehn

USDA/Forest Service, Fort Collins, Colorado

Abstract. High rural concentrations of ozone (O_3) are thought to be either stratospheric in origin, advected from upwind urban sources, or photochemically generated locally as a result of natural trace gas emissions. Ozone is known to be transported vertically downward from the above-canopy atmospheric surface layer and destroyed within stomata or on other biological and mineral surfaces. However, here we report winter-time eddy correlation measurements of vertical O_3 flux above a subalpine canopy of *Picea engelmannii* and *Abies lasiocarpa* in the Snowy Range Mountains of Wyoming that indicate anomalous upward O_3 fluxes. Upward fluxes of 0.5 μg m^{-2} s^{-1} (11 kg km^{-2} day^{-1}) were routinely measured during the 1991-92 winter season. Decreasing O_3 concentration from several hours to several days that relate to increasing positive O_3 flux magnitudes and visa versa, suggest O_3 may be temporarily stored in the snow base.

Introduction

Forest ecosystems play a role in the uptake and destruction of tropospheric O_3. This role and the tropospheric O_3 budget in remote forested ecosystems is uncertain [Chameides and Lodge, 1992]. Ozone deposition, rapid during the growing season and slower during winter months [*Wesely*, 1983], is retarded further by surface snow cover [*Stocker et al.*, 1995]. Our data show the unexpected effect of snow cover on O_3 fluxes above a subalpine spruce-fir forest. In the presence of below-canopy surface snow they reverse direction from negative (downward) to positive (upward) [*Zeller and Hehn*, 1994]. Positive O_3 fluxes attributed to vertical entrainment of clean air from aloft have been measured by aircraft [*Lenschow et al.*, 1982] and modeled [*Gao and Wesly*, 1994] in the upper atmospheric boundary layer. Measurements of negative vertical O_3 profiles above forested canopies have lead to 'counter-gradient' O_3 flux claims assuming O_3 only deposits towards the Earth's surface [*Fontan et al.*, 1992; *Enders*, 1992; *Denmead and Bradley*, 1985]. Galbally and Allison [1972] reported wintertime upward ozone fluxes (1.6 μg m^{-2} s^{-1}) over fresh snow based on gradient measurements at 1807m in SE Australia.

Snowy Range hourly O_3 concentrations average 45 to 60 ppb year round [*Wooldridge et al.*, 1994], and are typical of clean high altitude rural sites [*Wunderli and Gehrig*, 1990]. The above-canopy diurnal O_3 concentration at this location does not exhibit the large day/night maximum/minimum pattern typical of urban, photochemically dominated air masses at any time during the year [*Wooldridge et al.*, 1994]. However, below-canopy, 3 m, summertime O_3 concentrations have a predominant day/night pattern: minimum values can drop to 10 ppb at night. Ozone concentrations appear to be horizontally uniform in the surrounding area: simultaneously daytime O_3 concentrations near Centennial, WY, 8 km southeast, during 1990 were within 1-2 ppb of those we measured at 3 m height and values measured at a U.S. EPA National Dry Deposition Site (NDDN) 10 m height, 400 m southwest of our Brooklyn Lake tower site during 1993 were within 1 ppb [*Wooldridge et al.*, 1994].

These positive O_3 flux measurements are unusual and deserve a critical examination. Here we describe the experiment and present the results of measured O_3 fluxes, concentrations, and summarized meteorological data collected during five periods in 1992. These periods contrast the O_3 flux difference between winter (snow cover) and summer (no snow cover) and capture the spring and autumn O_3 flux directional transitions.

Paper number 96GL00786

Methods

Site

Data were collected at the Brooklyn Lake tower site situated in an Engelmann Spruce - Subalpine Fir forest opening approximately 30 meters in diameter. The site is within the U.S.D.A. Forest Service's Glacier Lakes Ecosystem Experiment Site (GLEES) area in the Snowy Range of the Medicine Bow National Forest, Wy. The GLEES complex is described by Musselman [1994]. The 29 m Brooklyn Lake tower (base elevation 3,186 m, 41° 22'N, 106° 14.5'W) is approximately 3 km southeast of the Snowy Range ridge (3,460 m average elevation). The average forest stand height is 17 m with representative displacement height, d, 11.7 m and roughness length, z_o, 1.7 m. The terrain within 1 km of the tower slopes +2.5% from west to east and -9.7% from north to south. This site is relatively complex for eddy flux experiments, however concurrent measurements of momentum and sensible heat fluxes provided reasonable values. Fitzjarrald and Moore [1992] found scalar flux measurements in non-homogeneous regions were robust and representative of the upwind footprint. Upwind terrain in the predominant wind direction, west-northwest, is forested with a flat +2.2% slope for at least 1 km.

Flux Measurements

Ozone concentration and flux data presented were collected in 1992 during five distinct periods: April 16-26 with 1 m snow cover representing the subalpine winter environment; April 28 - May 4, beginning transition period with rapid snow melt; May 7-18, the transition period during the final days of spring snow melt; July 2-8, a subalpine summer scenario; and September 30 - October 7, during the autumn to winter transition.

The eddy correlation system [*Zeller et al.*, 1989] used to measure O_3, sensible heat, and momentum fluxes, O_3 concentrations, temperature and wind speed was employed at 23 m (6 m above canopy) on the Brooklyn tower. Standard meteorological sensors are permanently mounted at 10 and 29 m for routine GLEES measurements [*Musselman*, 1994]. The essential sensors for O_3 flux measurements are the uvw Gill anemometer and the chemiluminesence ambient air monitor (CAAM1) [Ray et al., 1986]. The CAAM1 was continuously calibrated using a TECO49 commercial UV adsorption instrument. Ambient air was sampled from the 23 m height through a 25 m length, 1.6 cm diameter teflon tube. The intake system lag time, t_l, was typically 2.4 s. A Gill uvw anemometer was used in place of a sonic anemometer for its greater durability in harsh alpine weather. The 13 Hz O_3 eddy deviations, $c' = c - \overline{c}$ ($\overline{c}$: 3 minute recursive filter average

concentration) and turbulent wind components u', v' and w', are multiplied then averaged over half-hour sampling periods [*McMillen*, 1986] to obtain the vertical flux, F_c ($\mu g\ m^{-2}\ s^{-1}$, equation 1) after a vector coordinate rotation for the $\overline{w} = 0$ streamline:

$$F_c = \overline{w'(t - t_l)c'(t)} \quad (1)$$

Here, negative F_c indicates downward flux. Sensible heat and momentum flux are obtained likewise. Coordinate rotations do not effect scalar flux sign and have a very small effect on measured flux magnitudes. Fluxes with associated streamlines within ±5° of horizontal account for 98% of the data presented here. Gill uvw anemometer data were corrected in real time for the inherent cosine response problem [*Massman and Zeller*, 1988]. The PRT fast response temperature sensor was routinely damaged by harsh weather hence sensible heat flux was also estimated (Table 1) using measured eddy diffusivities for momentum, assuming similarity with heat diffusivity and temperature lapse rate between 10 and 29 m, to provide directional and intensity comparisons with measured sensible heat and O_3 fluxes.

Businger's [1986] list of eddy correlation measurement concerns were used for data evaluation and editing. Ozone flux corrections [equation 12, *Luening and Moncrieff*, 1990] for vapor effects were insignificant ($\pm 1 \times 10^{-7}$ $\mu g\ m^{-2}\ s^{-1}$). Data below the scale height, $h_t < \left| \overline{w'c'} / (\partial \overline{c} / \partial t) \right|$ of 23 m were culled. A digital butterworth filter was applied in real time to account for aliasing. Instrument response and instrument separation corrections would typically increase flux magnitudes by 20 to 80% [*Zeller et al.*, 1989]. The latter do not effect the main result (O_3 flux direction), hence the flux data are presented here without those corrections as they would typically increase the magnitude of the upward O_3 fluxes slightly more than the downward. Order of magnitude and flux direction are not affected by the lack of these corrections and make the reported upward flux values conservative.

Neutral stability micrometeorological statistics for wind, temperature and O_3 are fairly consistent from period to period and equivalent to results from other field studies. For example σ_w/u_* was consistently 1 ± 0.2 compared to 1.3 for flat terrain. Dimensionless wind shear, $\phi_m = kz / u_* (\partial u / \partial z)$, was consistently 1.1 ± 0.3 where $u_* = \sqrt{-\overline{w'u'}}$ was calculated from the momentum flux. There are no aberrant values in Table 1 to indicate a sampling problem with either the sensors, the sampling system or the tower configuration.

Results

The eddy correlation measurements show consistent upward daytime O_3 fluxes during two snow-covered winter periods and downward fluxes during the growing season with the absence of snow cover. Half-hour average upward O_3 fluxes exceeded 0.5 $\mu g\ m^{-2}\ s^{-1}$ (11 $kg\ km^{-2}\ day^{-1}$) during April 14-27, 1992. These values are the same magnitude as the downward fluxes measured during July 1992 at the same location. Sign-change shifts in daytime O_3 flux movement patterns occurred during the 13-day May 6-19, 1992 sampling period snow-melt was completed, and again during the 8-day period in autumn when snow returned. There are several examples when nighttime O_3 flux does not cease as might be expected. On these occasions, lapse rate and wind data indicate neutral stability which allows for continued turbulent transport. Figs. 1 through 3 show O_3 concentrations, O_3

Table 1. Daily Ozone, Ozone Flux and Meteorological Values

Julian Day	O_3 Max/Min (ppb)	O_3 Flux Total ($mg\ m^{-2}$)	O_3 Flux Max ($\mu g\ m^{-2}\ s^{-1}$)	T Max/Min (°C)	RH Max/Min (%)	Heat Flux Max 1/2 hr (Watts m^{-2})	Heat Flux Estimate (Watts m^{-2})	Radiation Max (Watts m^{-2})	$\overline{u}$ ($m\ s^{-1}$) **	$\overline{u'w'}$ ($m^2\ s^{-2}$) **	$\overline{w}$ ($m\ s^{-1}$) **	$\overline{\theta}$ (Degree) **	Precip. (mm)	Snow (cm)
	23 m	23 m	23 m	29 m	29 m	23 m	23 m	29 m	23 m	23 m	23 m	23 m	1.5 m	
106	59 / 42	3	0.3	6 / -2	98 / 73	-	50e	830	1.8	-0.2	0.01	150	5	113
107	60 / 48	5	0.4	2 / -1	97 / 90	-	25e	640	3.1	-0.5	0.15	270	3	-
108	59 / 42	12	0.35	5 / -2	95 / 79	-	25e	770	9.2	-2.1	0.52	260	21	-
109	52 / 46	19	0.6	-4 / -9	96 / 93	-	15e	730	7.0	-1.8	0.25	300	25	-
110	49 / 40	17	0.42	-4 / -8	95 / 92	-	-	410	7.4	-1.5	-1.50	320	8	-
111	51 / 40	18	0.6	-1 / -9	95 / 75	-	10e	930	10.0	-2.8	-0.05	320	5	-
112	51 / 47	15	0.58	6 / -6	87 / 45	-	85e	1050	4.9	-1.0	0.17	290	0	-
113	57 / 46	19	0.51	4 / -2	94 / 65	-	50e	930	5.2	-1.1	0.37	280	5	-
114	65 / 51	14	0.3	-2 / -7	93 / 43	-	50e	810	8.9	-2.6	0.55	290	4	-
115	64 / 54	9	0.26	3 / -9	55 / 26	-	110e	980	6.8	-1.8	0.19	300	0	-
116	61 / 49	7	0.28	8 / -6	32 / 20	-	90e	960	3.0	-0.5	0.00	310	3	-
117	62 / 44	5	0.21	10 / -4	36 / 20	-	85e	970	4.3	-0.8	0.00	310	0	103
119	61 / 54	12	0.35	2 / 10	35 / 20	320	380e	980	4.5	-1.4	0.18	280	0	-
120	64 / 49	6	0.21	4 / 12	25 / 20	310	350e	960	4.0	-0.8	0.36	250	0	100
121	73 / 64	12	0.22	7 / 13	25 / 18	340	410e	1000	7.5	-2.0	0.52	240	0	-
122	67 / 36	15	0.65	2 / 9	96 / 21	250	450e	990	7.1	-1.9	0.44	260	0	-
123	60 / 46	4	0.19	-1 / 7	96 / 25	350	200e	1090	1.3	-0.1	-0.06	v.	3	-
124	62 / 50	2	0.08	2 / 9	32 / 19	340	280e	1000	2.2	-0.4	0.00	300	1	-
125	63 / 51	1	0.07	1 / 10	43 / 21	340	290e	1020	1.9	-0.3	0.00	300	0	-
126	60 / 51	2	0.08	3 / 10	60 / 29	340	200e	1010	2.3	-0.3	-0.16	340	0	-
128	55 / 47	3	0.2	13 / 1	69 / 33	400	300e	1050	3.7	-0.7	-0.05	310	4	45
129	55 / 41	-1	0.08*	11 / 2	92 / 45	90	50e	660	1.2	-0.1	0.05	210	0	-
130	56 / 44	5	0.6*	1 / 9	95 / 57	280	200e	810	5.0	-0.8	0.36	230	3	-
131	62 / 43	10	0.23	4 / -5	95 / 50	-	310e	1000	5.5	-1.8	0.33	270	0	-
132	51 / 45	5	0.8	9 / -1	85 / 35	-	350e	1000	8.4	-2.8	0.57	260	1	-
133	52 / 42	4	0.5	10 / 2	90 / 30	-	350e	990	5.3	-1.2	0.25	280	4	-
134	54 / 45	17	0.9*	7 / 0	99 / 70	-	25e	770	5.0	-1.2	0.28	270	8	-
135	54 / 46	-3	-0.11	10 / 1	90 / 33	-	260e	1000	5.0	-1.1	0.20	280	0	0
136	61 / 49	-2	-0.2*	12 / 3	60 / 30	-	290e	950	5.0	-1.1	0.40	250	0	0
137	58 / 46	4	-0.1	10 / 1	90 / 30	-	290e	980	6.8	-1.7	0.35	280	0	0
138	52 / 46	-5	-0.2	14 / 0	64 / 20	-	250e	1030	3.0	-0.5	0.26	250	0	0
139	57 / 49	-8	-0.27	16 / 4	55 / 19	-	240e	1060	3.5	-0.6	0.26	270	1	0
184	34 / -	-	-0.2	- / 1	- / 90	120	-700e	800	4.7	-1.1	0.15	295	5	0
185	54 / 37	-22	-0.6	12 / 2	95 / 39	320	250e	1000	5.0	-1.4	0.33	270	0	0
186	59 / 50	-18	-0.6	19 / 2	55 / 22	300	350e	1040	5.7	-1.6	0.42	245	0	0
187	48 / 35	-10	-0.3	19 / 9	42 / 20	290	300e	995	6.3	-1.8	0.43	255	0	0
188	42 / 30	-8	-0.28	19 / 9	48 / 28	300	390e	990	7.4	-2.3	0.50	270	0	0
189	53 / 33	-1	0.51	12 / 4	94 / 42	200	100e	760	7.1	-1.7	0.35	265	8	0
190	63 / 50	-23	-0.63	13 / 6	70 / 42	140	120e	660	3.9	-1.0	0.25	255	0	0
274	58 / 49	-5	-0.2	16 / 4	33 / 18	-	150e	770	1.8	-0.1	0.03	160	0	0
275	55 / 47	-5	-0.27	17 / 5	35 / 17	200	180e	750	2.0	-0.2	0.07	260	0	0
276	70 / 48	-3	-0.15	16 / 3	32 / 17	200	100e	750	3.9	-0.2	0.10	150	0	-
277	54 / 46	-4	-0.21	16 / 6	35 / 18	370	310e	740	3.9	-0.6	0.70	220	0	-
278	50 / 39	1	±0.15*	9 / 1	80 / 40	360	350e	735	5.3	-1.4	0.40	270	0	-
279	45 / 34	0	±0.08*	7 / -2	95 / 52	230	90e	750	3.0	-0.4	-0.08	140	0	-
280	50 / 27	-3	±0.4*	7 / -2	98 / 43	330	240e	730	4.5	-1.0	0.30	270	5	-
281	- / 25	2	±0.3*	-7 / -11	97 / 45	-	100e	760	5.9	-1.3	0.02	320	2	3

- Missing data or no measurement taken; * Positive and negative ozone flux on the same day;
e Estimated; v Variable; ** Midday (10:00-15:00 MST) average

fluxes and vertically integrated time rate of O_3 change for three of the five multi-day periods given in Table 1.

Table 1 summarizes the meteorological and O_3 data. Midday meteorological values are representative averages between 10:00 and 15:00 MST, the diurnal hours of greatest O_3 flux activity. Total O_3 flux was obtained by integrating half-hour values commencing midnight each day. The maximum daily deposition value, -23 mg m^{-2}, on Julian day (JD) 190 compares in magnitude to the maximum upward flux, 19 mg m^{-2} on JD 113. In addition to the presence of snow, ambient temperature appears to effect O_3 flux direction. Between 5 to 10 °C, O_3 fluxes can be either up or down, below 5 °C they are mostly positive, and above 10 °C they are mostly negative. Ozone flux direction is neither effected by vertical wind speed or direction nor horizontal wind direction; both would indicate a terrain induced bias.

Fig. 1, April 14 - 27, 1992 (JD 106-117), shows the day-to-day consistency of the upward O_3 fluxes. Temperatures ranged from 10 °C to -9 °C during this period. Ozone fluxes reached 0.6 μg m^{-2} s^{-1}. The April 29 - May 4, 1992 (JD 119 - 126) period (Table 1) shows a decrease in O_3 flux after JD 123. This change was preceded by a sharp drop in O_3 concentration associated with a simultaneous jump in O_3 flux followed by sustained lower wind speeds. Temperatures ranged from -1 (occurred briefly midnight JD 123) to 13 °C. May 6-19, 1992 (JD 127-140), covers the period snowmelt ended and the daytime O_3 flux direction switched from upward to downward. Ozone fluxes ranged from positive to negative during this period but remain predominately negative after JD 138. Temperatures ranged from -5 to 16 °C (below zero values were brief nighttime excursions on JD 131-2) Fig. 2, July 2-9, 1992 (JD 184-191), shows the typical negative O_3 fluxes that occur during growing seasons. The downward diurnal flux pattern was briefly interrupted on JD 189 when it rained 0.3 mm. This is the only incident when positive O_3 flux was directly correlated with a precipitation event. Similar brief summertime events have been reported by Enders [1992] and Kelly and McTaggart-Cowen [1968]. Temperatures during this period ranged from 1 to 19 °C but remained below 7 °C on JD 189. Fig. 3, September 29 - October 8, 1992 (JD 274-281), shows the transition from negative daytime O_3 fluxes to positive fluxes. During this period, temperatures dropped below 0 °C and RH increased from 30 to 80% as O_3 fluxes turned positive. Based on meteorological data it is likely snow flurries started JD 278 with snow accumulating on the ground by JD 279. Prior to JD 278 daytime temperatures ranged from 3 to 17 °C.

Discussion

Upward fluxes suggest either surface or canopy emissions of O_3 and/or in the case of complex terrain, horizontal and/or vertical advection of O_3. The potential contributions of local O_3 production (or destruction), R, and advection below 23 m can be roughly estimated from the measured data by vertically integrating the equation for O_3 conservation from the surface to measurement height. Using the average wind streamline

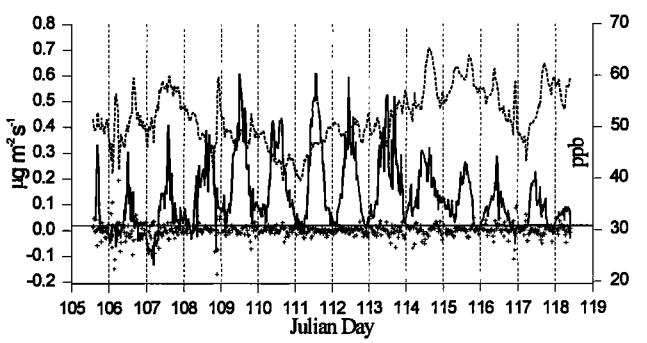

Figure 1. Half-hour average O_3 concentration (dashed) in parts per billion (ppb), O_3 flux (solid lines) and vertically integrated time rate of O_3 change (+) in μg m^{-2} s^{-1} for the period April 14 to 27, 1992.

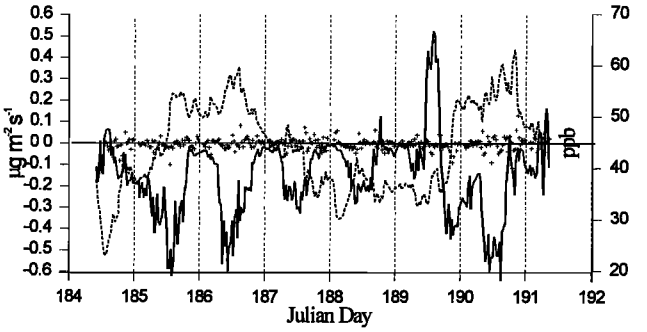

Figure 2. Half-hour average O_3 concentration (dashed) in parts per billion (ppb), O_3 flux (solid lines) and vertically integrated time rate of O_3 change (+) in μg m^{-2} s^{-1} for the period July 2 to July 9, 1992.

($\overline{w}=\overline{v}=0$), assuming $w'c'_o = 0$, and neglecting molecular diffusion gives equation 2.

$$\int_0^{23m} \frac{\partial \bar{c}}{\partial t}\delta z + \int_0^{23m} \frac{\partial \overline{w'c'}}{\partial z}\delta z = -\int_0^{23m} u\frac{\partial \bar{c}}{\partial x}\delta z - \int_0^{23m} \frac{\partial \overline{u'c'}}{\partial x}\delta z - \int_0^{23m} \frac{\partial \overline{v'c'}}{\partial y}\delta z + \int_0^{23m} R\delta z \qquad (2)$$

As seen in Figs. 1 - 3 the vertical flux (second term, equation 2) is at least an order of magnitude greater than the local time rate of change (first term) hence the local time rate of change does not significantly contribute to the vertical flux. If horizontal advection (third through fifth terms) were insignificant, the positive vertical fluxes would be due to either locally generated O_3 (last term) or vertical advection term which was canceled to obtain equation 2. Given the presumed lack of O_3 precursors in this wintertime scenario it is unlikely O_3 is generated locally and vertical advection does not seem a likely explanation given the lack of correlation between flux direction and $\pm\overline{w}$. (Table 1). Horizontal advection is an unlikely contributor based on measurement comparisons between our site, the NDDN site and the Centennial, WY site, suggesting the horizontal gradient terms are also very small. This leaves R indicating either $w'c'_o$ is not zero as assumed and/or the existence of a negative vertical O_3 profile at measurement height.

Atmospheric boundary layer O_3 usually requires nitric oxide (NO), nonmethane hydrocarbons and ultraviolet energy to drive its photochemical production [*Olszyna et al.* 1994]. Forests are sources of natural nonmethane hydrocarbons, which are known precursors for O_3 production and a possible cause of higher rural O_3 concentrations. Concentrations of nitrous oxide (N_2O) above typical ambient levels have been measured under and above the snow cover at GLEES [*Sommerfeld et al.*, 1993]. Since the same microorganisms which generate N_2O also generate NO [*Hutchinson and Davidson*, 1993], the possibility of an NO source during winter months exists, however the likely concentration is very low.

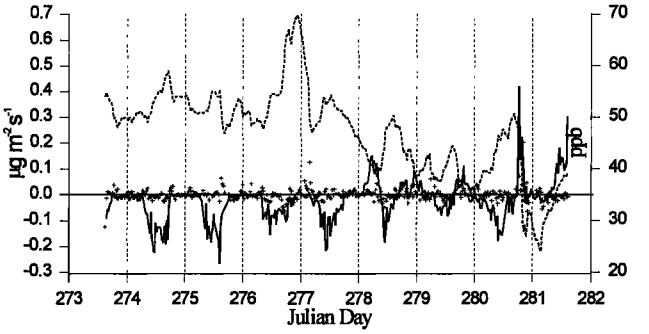

Figure 3. Half-hour average O_3 concentration (dashed) in parts per billion (ppb), O_3 flux (solid lines) and vertically integrated time rate of O_3 change (+) in μg m^{-2} s^{-1} for the period September 30, 1992, to October 7, 1992.

Galbally and Allison [1972] speculated O_3 might absorb on fresh snow without total destruction, however we suggest adsorption is more likely. Laboratory experiments indicate O_3 adsorption to ice reaches saturation quickly (< 1 s) with no further uptake [*Dlugokencky and Ravishankara*, 1992]. Using 50 ppb O_3 (9×10^{11} molecules cm^{-3}), an O_3 to ice sticking coefficient of 0.001 (range 0.01 - 0.0001) [*Dlugokencky and Ravishankara*, 1992] and 3×10^4 cm s^{-1} for O_3 molecular velocity, we estimate the rate of O_3 adsorption to snow to be 2.7×10^{16} molecules cm^{-2} s^{-1}. Taking 9×10^7 cm^2 m^{-3} as the specific surface for fresh snow [*Sommerfeld and Rocchio*, 1993] and accepting O_3 saturation within 1 s, there are potentially 2.4×10^{20} O_3 molecules m^{-3} in a 1 m snow base. It would take 4.5 days (range 0.5 - 45 days) to expel this O_3 assuming a constant flux of 0.5 μg m^{-2} s^{-1}. Larger downward O_3 fluxes are typically associated with higher O_3 concentrations as seen in Fig. 2. Fig 1. however, shows O_3 concentrations decreasing with increasing positive flux for several days, then decreasing with increasing concentrations for the next few days. On JD 122, a sudden drop in O_3 is associated with a sharp increase in upward O_3 flux. Given an equilibrium between ambient O_3 concentrations and ice surface saturation, this inverse behavior adds credence to the possibility O_3 is temporarily stored in the snow field and released by turbulent air interactions through the porous snow interface.

The delineating factor for upward versus downward O_3 fluxes appears to be snow cover and (to a lesser extent) ambient temperature. Both are environmental factors that potentially affect stomatal function. The measured fluxes are usually diurnal in nature reflecting daytime turbulent O_3 mass transfer. Some measurements show continued but weaker upward O_3 fluxes during nights with strong winds. Tree physiology also appears to play a role as the spring and autumn transition between positive and negative O_3 fluxes occurs around 5°C, a minimum ambient temperature for conifer growth [*Prentice et al.*, 1992].

Conclusions

The O_3 flux data measured by eddy correlation at the GLEES Brooklyn tower, Snowy Range, Wy, show reasonable summer growing season deposition (-0.5 μg m^{-2} s^{-1}). During winter and non growing seasons, upward O_3 fluxes were measured. The late winter upward fluxes are the same magnitude as the summer downward fluxes. As O_3 does not readily deposit on snow, the measured rate of O_3 deposition is expected to decrease during the winter but not reverse direction. The flux directional transition is apparently seasonal. The explanation for the upward O_3 fluxes remains unknown but suggest either: (1) the possibility of O_3 stored in the surface snow base; or (2) negative O_3 profiles above the forest canopy.

References

Businger, J.A. Evaluation of the accuracy with which dry deposition can be measured with current micrometeorological techniques. *J. Clim. & Appl. Meteor.*25, 1100-1124, 1986.

Chameides, W.L. and J.P. Lodge, Tropospheric ozone: formation and fate, in *Surface Level Ozone Exposures and their Effects on Vegetation* edited by A.S. Lefohn,.pp. 5-20, Lewis Pub., Chelsea, MI. 5-30, 1992.

Denmead, O.T. and E.F. Bradley, Flux-gradient relationships in a forest canopy, in *The Forest-Atmosphere Interaction.* edited by Hutchison, B.A and B.B. Hicks, pp. 421-442, D. Reidel, Boston, Mass.

Enders, G. Deposition of ozone to a mature spruce forest: measurements and comparison to models, *Env. Poll.*, 75, 61-67, 1992.

Fitzjarrald, D.R. and K.E. Moore, Turbulent transports over tundra. *J. Geophys. Res.*, 97:D15, 16717-16729, 1992.

Fontan, J, A. Minga, A. Lopez and A. Druilhet, Vertical ozone profiles in a pine forest. *Atm. Env.* 26A, 863-869, 1992.

Galbally, I. and I. Allison, Ozone fluxes over snow surfaces. *J. Geophys. Res.*, 77:21, 3946-3949, 1992.

Gao, W. and M.L. Wesely, Numerical modeling of turbulent fluxes of chemically reactive trace gases in the atmospheric boundary layer, *J. Appl. Met.*, 33, 835-847, 1994.

Hutchinson, G.L. and E.A. Davidson, Processes for production and consumption of gaseous nitrogen oxides in soil, in *Agricultural ecosystem effects on trace gases and global climate change*, pp. 79-93, Spec. Pub. 55. American Society of Agronomy, 1993.

Kelly, J.J., Jr. and J.D. McTaggart-Cowen, Vertical gradient of net oxidant near the ground surface at Barrow, Alaska, *J. Geophys. Res.*, 73, 3328-3330, 1968.

Lenschow, D.H., R. Pearson, Jr. and B.B. Stankov, Measurements of ozone vertical flux to ocean and forest, . *J. Geophys. Res.*, 87:Cll, 8833-8837, 1982

Leuning, R. and J. Moncrieff, Eddy-covariance CO_2 flux measurements using open- and closed-path CO_2 analyzers: corrections for analyzer water vapour sensitivity and damping of fluctuations in air sampling tubes. *Bdy. Lyr. Met.*, 53, 63-76, 1990.

Massman, W.J. and K.F. Zeller, Rapid method for correcting the non-cosine response errors of the Gill propeller anemometer, *J. Atm. and Oc. Tech.*, 5:6, 862-869, 1988.

McMillen, R.T., A BASIC program for eddy correlation in non-simple terrain, *Tech. Rep. ERL ARL-147*, 32 pp., NOAA ATDD Lab., Oak Ridge, Tenn., 1986.

Musselman, R. C., (Ed.), The Glacier Lakes ecosystem experiments site (GLEES): an alpine global change research study area, *Tech. Rep.RM-249*, 94 pp., U.S.D.A. Forest Service RMFRES, Ft. Collins, Colo., 1994.

Olszyna, K.J., E.M. Bailey, R. Simonaitis and [Others], O_3 and NO_y relationships at a rural site, *J. Geophys. Res.*, 99:D7, 14557-14563, 1994.

Prentice, I.C., C. Wolfgang, S.P. Harrison, R. Leemans, R.A. Monserud and A.M. Solomon, A global biome model based on plant physiology and dominance, soil properties and climate, *J. Biogeography*, 19, 117-134, 1992.

Ray, J.D.; D.H. Stedman and G.J. Wendel, Fast chemiluminescent method for measurement of ambient ozone, *Anal. Chem.*, 58, 598-600, 1986.

Stocker, D.; K. Zeller and D. Stedman, O_3 and NO_2 fluxes over snow measured by eddy correlation, *Atm. Env.*,.29:11, 1299-1305, 1995.

Sommerfeld, R.A., A.R. Mosier and R.C. Musselman, CO_2, CH_4, and N_2O flux through a Wyoming snowpack and implications for global budgets, *Nature*, 361, 140-142, 1993.

Sommerfeld, R.A. and J.E. Rocchio, Permeability measurements on new and equitemperature snow, *Water Res.*, 29:8, 2485-2490, 1993.

Wesely, M. L., Turbulent transport of ozone to surfaces common in the eastern half of the United States; in *Advanced Science Technology: 12*, pp. 345-370, Wiley, N.Y., N.Y., 1983.

Wooldridge, G.L., K.F. Zeller and R.C. Musselman, Ozone concentration characteristics in and over a high-altitude forest, 23rd Int'l Conf. for Alpine Met., Lindau, Germany, Sept 5-9, 1994.

Wunderli, S. and R. Gehrig, R., Surface ozone in rural, urban and alpine regions of Switzerland, *Atm. Env.*, 24A:10, 2641-2646, 1990.

Zeller, K.; W. Massman, D. Stocker, D. and [others], Initial results from the Pawnee eddy correlation system for dry acid deposition research, *Gen. Res. Pap. RM-282*, 44 pp., U.S.D.A. Forest Service RMFRES, Ft. Collins, Colo., 1989.

Zeller, K. and T. Hehn, Wintertime anomalies in ozone deposition above a subalpine spruce-fir forest, *Proc. 4th U.S.D.A Forest Service S. Sta. Chem. Sc.: Research and Applications of Chemical Sciences in Forestry*, 131-138, Feb. 1-2, 1994.

K. Zeller and T. Hehn, USDA/Forest Service, 240 West Prospect, Fort Collins, Colorado 80526.

(Received December 21, 1994; revised July 13, 1995; accepted February 6, 1996.)